

# Modulus Reconstruction by Simultaneous Data Response of Surface Stress and Strain Distribution

Md. Taslim Reza<sup>1</sup>, Muhammad Rezaul Hoque Khan<sup>2</sup> and Mohammad Rakibul Islam<sup>3</sup>

<sup>1,2,3</sup>Electrical and Electronic Engineering Department, Islamic University of Technology, Board Bazar, Gazipur, Bangladesh.

## Abstract

Medical imaging is vital to modern clinical practice, enabling clinicians to examine tissues inside the human body non-invasively. Its value depends on accuracy, resolution, and the image property (e.g., density). Various new scanning techniques are aimed at producing elasticity images related to mechanical properties (e.g., stiffness) to which conventional forms of ultrasound, X-ray and magnetic resonance imaging are insensitive. Elastography, palpography or strain imaging has been under development for almost two decades. Elasticity images are produced by estimating and analysing quasistatic deformations that occur between the acquisitions of multiple ultrasound images. Likely applications include improved diagnosis of breast cancer (which often presents as a stiff lump), but the technique can be unreliable and difficult to perform. In this paper a novel algorithm is proposed to find out the stress distribution from the strain distribution and stress value on the top surface of the Region of Interest (ROI). The comparison is also shown between the classical and the proposed method. Practical imaging is based on freehand scanning, i.e., the ultrasound probe is moved manually over the surface of the tissue. This requires that elasticity images are calculated fast to provide a live display, and the images need to present meaningful elasticity data despite the poorly controlled properties of the deformations. Stress distribution reconstruction is vital to find out the true value of the modulus distribution. Stress distribution only can predict based on different parameters. The modulus prediction error is minimized with a less number of iteration by using the proposed algorithm. It shows that only 6 iterations make the prediction error very close to 5% where as in conventional method it shows more than 12%.

## Key words:

*Modulus reconstruction, simultaneous data, distribution*

## 1. Introduction

Breast cancer is one of the most common causes of death from cancer in the United States. The American Cancer Society estimates that in 2007, approximately 180 510 new cases of invasive breast cancer will be diagnosed in the U.S. alone, and 40 910 deaths (40 460 women and 450 men) from this disease are predicted [1]. The lifetime probability of developing breast cancer in the next 10 years is evaluated as 13.2% [2]. A critical key to a continued reduction in mortality is easy detection and accurate diagnosis [3] made in a costeffective manner [4].

Current methods of breast pathology assessment include clinical breast examination (CBE), mammography, ultrasound, magnetic resonance imaging (MRI), and biopsy. Recent largescale clinical study of diagnostic performance of mammography for breast-cancer screening showed that diagnostic accuracy of digital and film mammography is only 78% and 74%, respectively [5]. According to data from the behavioral risk factor surveillance system, only 54.9% of U.S. women in 2003 have had a mammogram within that year [2]. Many indications for clinical breast MRI are recognized, including resolving findings on mammography and staging of breast cancer [7]. Dynamic contrast-enhanced MRI (DCE-MRI) has been demonstrated to provide a good sensitivity and specificity for differentiation of benign versus malignant lesions, due to altered angiogenesis mechanisms in tumors [3]. However, in addition to being costly, DCE-MRI requires injection of exogenous contrast agents to provide such contrast. An alternate imaging technique for breast cancer detection employs tissue stiffness as contrast mechanism. The technique is founded on the fact that alterations in breast tissue stiffness are frequently associated with pathology [4], [5]. This was demonstrated by stiffness measurement studies of ex vivo breast tissue samples conducted by Krouskop et al. [6] and Samani and Plewes [7], [8]. Based on their measurements, there is a significant difference between the Young's moduli of breast tumor and healthy breast tissues. As such, imaging breast tissue stiffness or breast elastography can be potentially used as a non-invasive breast cancer diagnosis method with a high efficacy. After development of elastography techniques [9], breast elastography was introduced as one of the first reported clinical applications developed based on the elastography concept. Two alternative methods of quasi-static and harmonic elastography were proposed. In the quasi-static methods, the tissue is mechanically stimulated very slowly and the resulting tissue deformation data are acquired using imaging modalities such as MRor ultrasound (US). In harmonic elastography, a mechanical wave is induced in the tissue and either vibration amplitude or wave speed is measured using MRI or US imaging techniques. In both cases, acquired data is used to

estimate the tissue mechanical properties (e.g., Young’s modulus).

Several feasibility studies [10]–[14] aiming at breast cancer diagnosis which involved harmonic US elastography were re-ported. Among relevant groups, Sinkus et al. [15], [16] and Van Houten et al. [17] proposed harmonic MR elastography techniques to measure the viscoelastic shear properties of in vivo breast lesions. While harmonic elastography techniques provide information related to tissue viscosity properties that may potentially carry more diagnostic information to characterize a breast lesion, they usually require additional hardware attachments for wave generation in addition to ad hoc software including specialized pulse sequences for MR elastography. These techniques also involve approximations which lead to elastic modulus reconstruction formulation based on the wave form and propagation characteristics. Other groups developed quasistatic elastography methods in the form of mechanical imaging [13], strain imaging [11]–[15] and full inversion techniques [5], [7] for breast cancer diagnosis. In mechanical imaging [13], mechanical parameters of the breast lesions were estimated using contact stress patterns on breast surface measured through a force sensor array pressed against the breast. This imaging approach is based on the premise that temporal and spatial changes in the stress pattern allow detection of internal structures with different elastic properties and assessing their geometrical characteristics. Strain imaging is based on a simplifying assumption of uniform tissue stress distribution under which tissue stiffness is proportional to its strain reciprocal. Since stress spatial variation developed within the breast tissue during mechanical stimulation is far from uniform, strain imaging does not provide reliable quantitative tissue stiffness information necessary for high sensitivity and specificity in breast cancer diagnosis. Full-inversion based elastography techniques on the other hand, account for tissue stress variation, permitting reconstruction of quantitative maps of elasticity modulus. One difficulty with in- version based quasi-static elastography methods is that they are computationally intensive, unstable and hard to implement. To reduce the complexity of the elastography inversion algorithms, Samani et al. [8] developed a MR-based iterative inversion algorithm for breast elastography. This technique was later implemented based on an ultrasound platform [9] as a step to develop near real-time, low cost and widely available imaging system. The algorithm was shown to be robust, however, it requires image segmentation for healthy and tumor tissue delineation. This requirement is not easy to fulfill, especially with US imaging.

In this paper, the methodology for unconstrained full inversion-based breast elastography considering the surface pressure of the top surface of the field of view

(FOV) is presented. In this work we show that, to predict the proper stress distribution throughout the experimental object, the surface pressure data guide to get the modulus data more precise and within less amount of iteration. Which give real advantage to get more accurate quantitative modulus data and the characteristics of the tumor. On the other hand this approach helps to converge to a satisfactory level in less computation.

## 2. Proposed Algorithm

The proposed method was developed assuming that the tissue is linear elastic and isotropic undergoing small deformation. Fig. 1. shows the steps with the flow chat. As such, the following equation, which is derived from Hooke’s law, governs each point in the tissue domain:

$$E = \frac{\sigma}{\epsilon} \tag{1}$$

In this equation  $\epsilon$  and  $\sigma$  denote the tissue strain and stress developed under mechanical stimulation, respectively. The tissue was assumed to be a near-incompressible material, hence tissue’s Poisson’s ratio 0.49 was employed in the reconstruction. The reconstruction technique is iterative as the YM followed a  $E_{i+1} = f(E_i)$  recursive formulation used in each iteration, where  $f$  involves strain calculation using finite element method. In this approach we assume the tissue elasticity uniformity throughout the volume of each of the normal and pathological tissues.

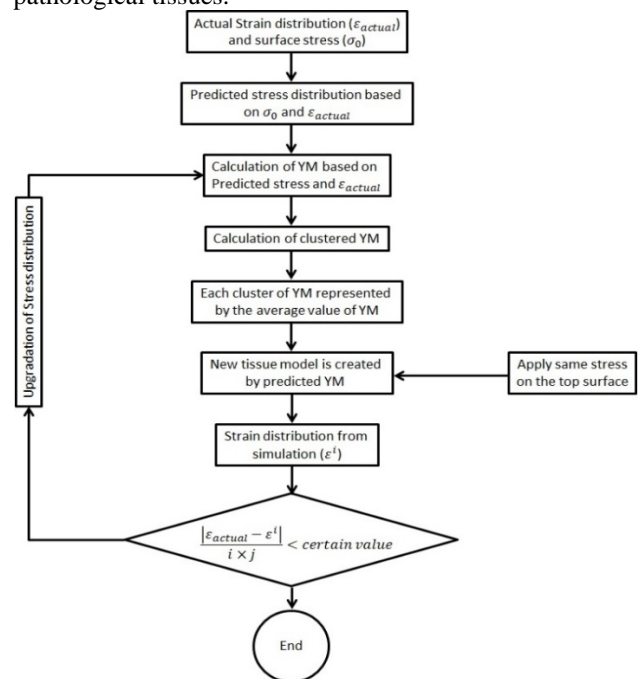


Fig 1: Flowchart illustrating the YM reconstruction procedure using surface stress.

Our algorithm follows the following steps:

- 1) Actual Strain distribution will be calculated from pre and post compression US data. At the same time, only the upper surface stress data will be collected by the 1D pressure sensor attached with the US probe.
- 2) First predicted stress distribution is calculated based on the surface known stress and known strain distribution,  $\epsilon_{\text{actual}}$ .
- 3) First YM distribution is calculated based on the first predicted stress distribution and known strain distribution ( $\epsilon_{\text{actual}}$ ) using Hooks law.
- 4) The YM is clustered for a defined number of clusters based on the structure of the tissue viewed in the B-mode image.
- 5) Then the full cluster is replaced by the average value of that clusters YM.
- 6) Simulated tissue model is created based on previous step. Same amount of stress is placed on the top surface for this simulated model.
- 7) From the simulated model, directly the strain distribution ( $\epsilon^i$ ) is collected.
- 8) The error distribution value of the strain is calculated compared with the actual strain ( $\epsilon_{\text{actual}}$ ) to the simulated strain distribution (explained in the previous step).
- 9) Strain distribution is updated based on the error distribution of the strain value  $\Delta$ , actual strain value and top surface stress value.

## 2.1 Finite Element Modelling

A model of breast tissue is created using COMSOL Multiphysics software. COMSOL Multiphysics is a cross-platform finite element analysis, solver and multi-physics simulation software [3]. It allows for the creation of a conventional physics-based user interface. The size of the overall model is taken as 3 cm with and 3.6 cm depth. The tumor is modeled by 1 cm diameter circular structure and placed in different positions for analysis. Skin and fat tissue depth is taken as 0.1 cm and 0.5 cm respectively where the width is 3 cm.

Water is the selected material used to represent various parts of the model. Distinctions were made between soft tissue, tumor, skin and fat by varying the mechanical properties. The altered properties included the Poisson's ratio and Young's modulus according to the literature [14]. Poisson's ratio is the ratio of the proportional decrease in a lateral measurement to the proportional increase in length in a sample of material that is elastically stretched. Young's modulus is a measure of the ability of a material to withstand changes in length when under lengthwise tension or compression. Sometimes referred to

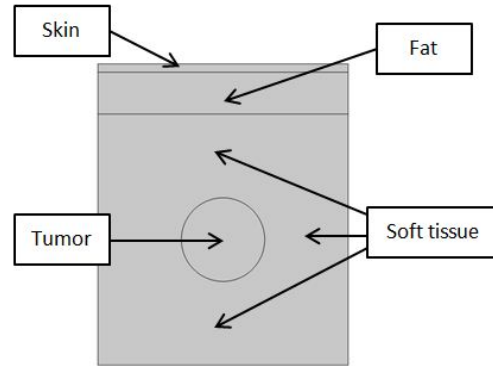


Fig. 2. Geometry of the FE model of breast tissue

Table 1: Mechanical properties of tissue components of breast

Tissue type	Poisson's ratio	Young's modulus
Soft tissue	0.495	10 kPa
Tumor	0.495	40 kPa
Skin	0.495	200 kPa
Fat	0.495	1.5 kPa

as the modulus of elasticity, Young's modulus is equal to the longitudinal stress divided by the strain. Poisson's ratio is taken as 0.495 for soft tissue, tumor, skin and fat. Young's modulus is considered as 10 kPa, 40 kPa, 200 kPa and 1.5 kPa for soft tissue, tumor, skin and fat respectively. It is assumed that bone is at that side. All the other sides were left free for movement.

For Young's Modulus reconstruction, stress and strain values are required. In a practical scenario, compression is made by the ultrasound probe. The stress field is usually non-uniform, so strain data are ambiguous, but strain imaging is the simplest way of displaying quasistatic deformation data to provide a visual indication of variation in mechanical properties [7, 15]. In our model we utilizes a fixed displacement of 0.03 cm to represent the compression from an ultrasound probe.

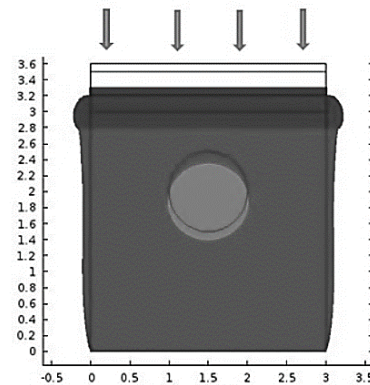


Fig. 3. Ultrasound probe is pressed at the top surface which is represented by fixed displacement of 0.03 cm

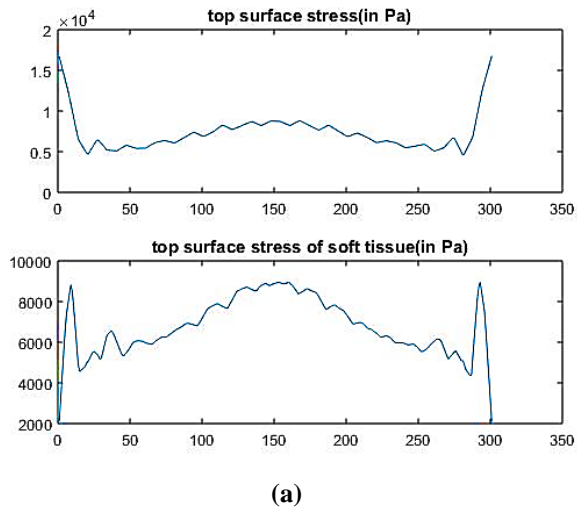
### 2.2 Estimation of Stress and Modulus

From simulated data, the top surface stress ( $\sigma_0$ ) and the strain distribution ( $\epsilon_{actual}$ ) is taken and exported to MATLAB for further modulus prediction. In practical case, strain distribution can be calculated from pre and post compressed data collected by US machine, where there will be a pressure sensor attached with the probe and it will give the surface stress distribution. The distribution of the stress ( $\sigma$ ) is predicted based on both the top surface stress and change of strain distribution value (Equation 2). To avoid complexity, we assume that the surface stress distribution is closely equal to just under the fat tissue. This assumption is also justified by the simulation result (Fig. 4.). For predicting stress distribution, the area under the fat to the lower most point is considered. Otherwise there are some unwanted error in the prediction due to the sharp change of the characteristic of skin to fat and fat to normal tissue.

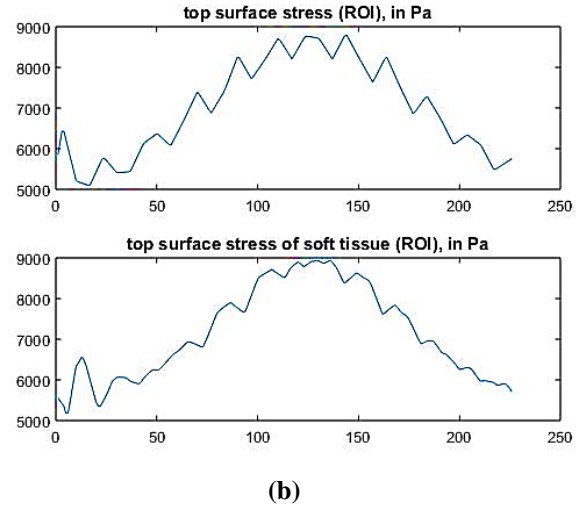
$$\sigma^{i_0+1,j} = \sigma^{i_0,j} * \alpha * |\epsilon^{i_0+1,j} - \epsilon^{i_0,j}| \quad (2)$$

### 2.3 Error Estimation

By using equation 1 and 2, the first modulus value is predicted. The predicted modulus value is clustered in different value. Based on the cluster modulus data found in the MATLAB environment FEM structure is created in the COMSOL for the first iteration. On that new model the same amount of displacement is created on the top surface of the structure. Since this structure is created based on the predicted stress profile, it will not provide the actual strain distribution. Scattered strain data is imported to MATLAB again and converted to matrix data. This is the first error strain data. In this phase, the actual strain data is compared with the first error strain data. In the second iteration, the challenge is to predict the stress value for each point based on the previously predicted stress value and the first strain error distribution.



(a)



(b)

Fig. 4. Stress distribution along to the surface of the structure and to the surface of the soft tissue. (a) Showing the full width, (b) showing the ROI section only.

$$\sigma^{i,j} = \sigma^{i-1,j-1} * \beta * (\epsilon_{actual}^{i,j} - \epsilon_{error(1)}^{i,j}) \quad (3)$$

Here  $\sigma^{i,j}$  is the new predicted stress value and it is based on the previously predicted stress,  $\sigma^{i-1,j-1}$  and a percentage of deviation of the strain value,  $\beta$ . Empirically  $\beta$  should be selected to get less strain error in the next iteration and hence need less iteration to converge.

This newly predicted stress value along with the surface stress and actual strain distribution is taken as the input to find the next modulus distribution ( $E_{predicted}$ ) based on the Hooke's law. After finding the predicted modulus in the second phase the same Gaussian filter is applied to get the smooth modulus distribution. Using the K-mean clustering algorithm, modulus values are clustered and distinct regions are created. Each of the regions is presented by a single modulus value as it done in the last phase. Now again the FEM structure is created based on the modulus value found in the MATLAB platform. The Same amount of displacement is applied on the top of the tissue structure and new strain distribution is found ( $\epsilon_{error(2)}^{i,j}$ ). Then the stress value is updated according to equation (4) and this process is repeatedly done as long as it converges to a particularly targeted deviation,  $\Delta$ . Here,

$$\Delta \leq \frac{|\epsilon_{actual}^{i,j} - \epsilon_{error(n)}^{i,j}|}{\epsilon_{actual}^{i,j}} * 100\% \quad (4)$$

where, n is the number of iteration needed to converge.

### 3. Result and Discussion

In case of conventional elastography imaging, the compression pressure or stress is not considered for

modulus reconstruction. Mostly in strain imaging, only the strain data is considered to get an idea of the distribution of the variation of the modulus. In this paper, surface stress made by the ultrasound probe is taken as the additional information to predict the stress distribution hence to predict the modulus. In COMSOL a fixed displacement is created to simulate the pressure on the surface and the stress data is taken from the top surface. From the FEM structure, the strain data is exported to the MATLAB for the whole structure. At first, it is a scattered data which is difficult to handle. So it is converted to matrix data to make the calculation easy. Based on the surface stress data and strain data the modulus value is being predicted. For this Hooke's law is the governing theory. In this phase the surface stress value is taken as it is. For all other stress values, it is calculated based on the surface stress and a certain percentage of change of strain value as stated in equation (3).

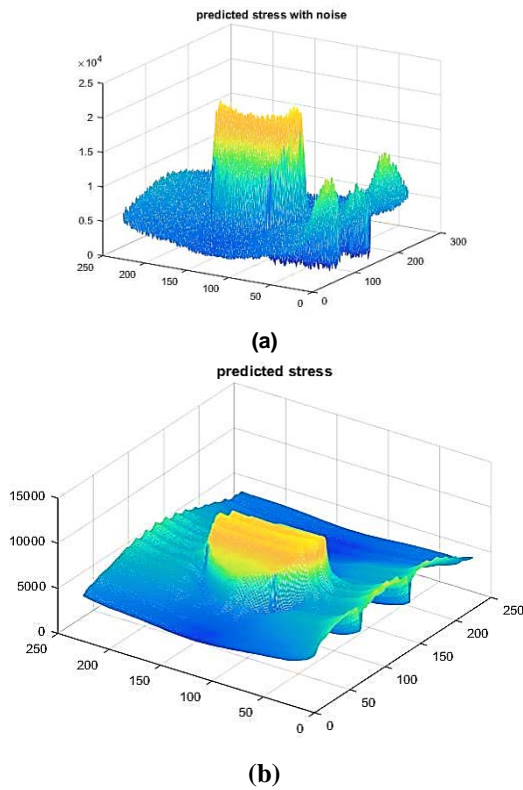


Fig. 5. (a) First predicted stress with noise, (b) first predicted stress by applying Gaussian filter.

It is been observed that due to the skin and the fat layer, the first predicted modulus values suffers by mentionable errors. It is also important to mention that the stress value and the stress profile just under the fat tissue or very specific, on the top surface of the soft tissue are almost the same which is mention in the last section. So the top surface stress of the soft tissue is taken as the surface

stress. This will help to give good prediction result from the very first step. For this reason, soft tissue along with the tumor is selected as the ROI for predicting modulus and updating the stress value.

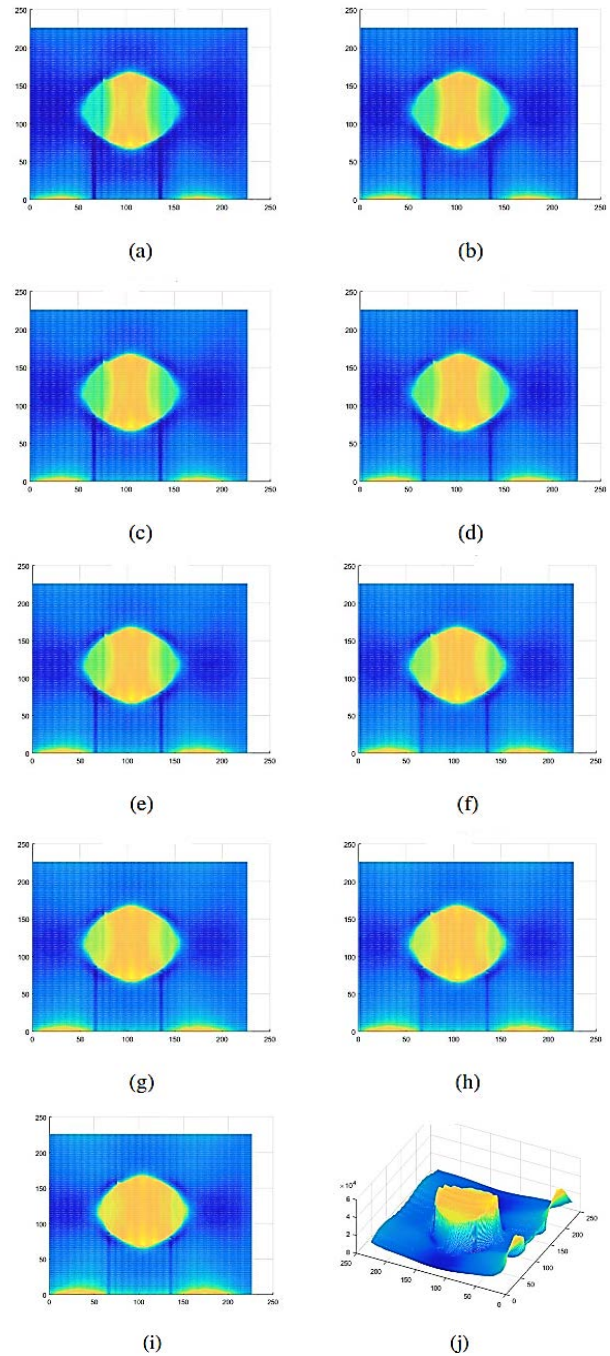


Fig. 6. (a) to (i) shows first to ninth iterated predicted modulus distribution respectively, (j) is the 3 D view of the ninth iterated predicted modulus distribution.

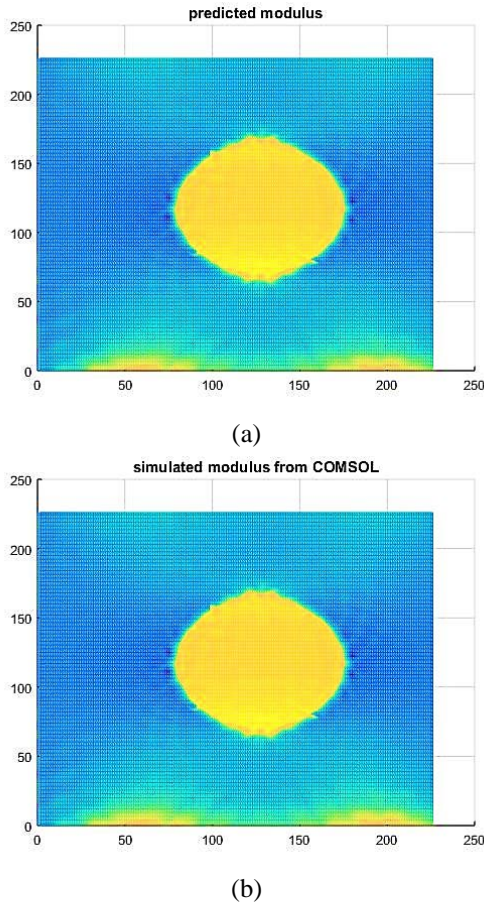


Fig. 7. (a) is the predicted modulus distribution for  $\Delta \leq 1\%$ . (b) is the simulated modulus found from FEM model.

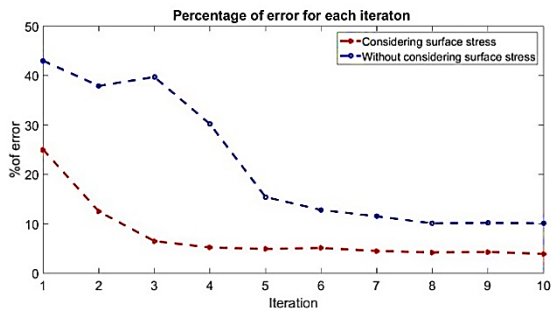


Fig. 8. Comparison of error in percentage of the modulus prediction for considering and without considering surface stress.

For calculating the modulus distribution, this predicted stress based on the surface stress and strain distribution is taken. It is observed that there is some sharp change in the first predicted stress distribution (Fig. 5). Which is not practical. Different filtering option is tried and Gaussian filter is applied to resolve the unwanted predicted modulus problem [12]. This filtering helps to smooth the

predicted value. For the Gaussian filter, the standard deviation is taken as 1 empirically.

First stress distribution is predicted based on the equation 2, where  $\alpha$  is taken as 0.5 empirically. According to the Hooke’s law modulus distribution is calculated. This ends the first iteration. For the second step, the distribution of the first predicted modulus value is clustered by using K-mean clustering algorithm. And two distinct area is selected for the next processing in COMSOL. Here each cluster is filled with the average value of that cluster. Which represents the modulus value input for the next iteration.

For the next iteration, this structure is taken as the input of the COMSOL where the same amount of displacement is applied on the top of the surface. The strain value is exported to MATLAB for next step calculation. At this stage, the stress value is updated based on the equation 4 where  $\beta$  is taken as 0.3 or 30%. The predicted modulus is calculated as in the first step. This completes the second iteration. The same steps are followed as long as the deviation of the strain distribution ( $\Delta$ ) is equal to or less than a certain level. In this case,  $\Delta$  is taken as 1% which leads the modulus average error less than 4%. Figure 3.6 – 3.8 shows all the outputs found during those iteration. For this example structure it takes ten iterations to the  $\Delta$  to 1%. The same process is executed for the new tissue structure with predicted modulus but the same displacement on the surface. Ten iterations is allowed for this modulus prediction since by using the proposed novel algorithm less than 1% strain error is reached by applying those number of iterations. Fig. 6 representing the predicted modulus in each iteration. After each iteration a significant change in modulus value.

It is very significant that when the surface stress is considered then the prediction error becomes very close to 5% by only 6 iterations. After that only 2% error lessens for more 4 iterations. So if 5% error is satisfactory then only 6 iteration is enough for the final modulus prediction. Which will save a substantial time for reconstruction. As this is a very time-consuming process, it may consider for practical evaluation purpose. On the other hand, while surface stress is not considered, it provides a huge error for first 4 iterations. However, after 8<sup>th</sup> iterations, it gives a very constant modulus error which is around 10% (Fig. 8).

#### 4. Conclusions

In this paper, the proposed methodology is shown for unconstrained full inversion-based breast elastography considering the surface pressure of the top surface of the field of view (FOV). In this work, it is also shown that, to predict the proper stress distribution throughout the experimental object, the surface pressure data guide to get

the modulus distribution for more precise and take less computational time. Which give a real advantage to get more accurate quantitative modulus data and the characteristics of the tumor. On the other hand, this approach helps to converge to a satisfactory level in less computation.

This paper is carried out focusing on the development of an analytical model of the breast with the tumor which refers to the practical physiology of the breast tissue. The main focus of this dissertation is to develop a novel reconstruction algorithm to estimate stress distribution hence Young's modulus distribution by knowing the strain distribution and surface stress. The strain distribution can be found from pre and post compression RF data and surface stress can be found from the pressure sensor implanted on the surface of the US probe.

This paper contributes to a practical simulated model of the breast tissue section with the tumor which refers to the practical environment to test the proposed novel algorithm. For different aspects, this simulated model can be modified to test the outcome of the proposed algorithm in a complex situation. Apart from the simulation of the tissue structure, the hardware can be built to collect surface pressure of the tissue. The clinical data is needed for validating the algorithm.

### Acknowledgments

The authors express their gratitude to Dr. S. Kaisar Alam, Senior Member, IEEE, visiting Research Professor of the Center for Computational Biomedicine Imaging and Modeling, Rutgers University, the State University of New Jersey for contributing in this research.

### References

- [1] Worldwide Breast Cancer. [Online]. Available: [www.worldwidebreastcancer.com](http://www.worldwidebreastcancer.com), Accessed on: Jan. 25, 2017.
- [2] J. E. Joy, E. E. Penhoet, and D. B. Petitti, Institute of Medicine (US) and National Research Council (US) Committee on New Approaches to Early Detection and Diagnosis of Breast Cancer, *Saving Women's Lives: Strategies for Improving Breast Cancer Detection and Diagnosis*. Washington, DC, USA: Nat. Acad. Press, 2005.
- [3] S. C. Rankin, "MRI of the breast," *Brit. J. Radiol.*, vol. 73, no. 872, pp. 806–818, Aug. 2000.
- [4] Y. C. Fung, *Biomechanics: Mechanical Properties of Living Tissues*, 2nd ed. New York, NY, USA: Springer, 1981.
- [5] T. A. Krouskop, T. M. Wheeler, F. Kallel, B. S. Garra, and T. Hall, "Elastic moduli of breast and prostate tissues under compression," *Ultrason. Imag.*, vol. 20, no. 4, pp. 260–274, Oct. 1998.
- [6] A. Samani and D. Plewes, "An inverse problem solution for measuring the elastic modulus of intact ex vivo breast tissue tumours," *Phys. Med. Biol.*, vol. 52, no. 5, pp. 1247–1260, Mar. 2007.
- [7] B. S. Garra et al., "Elastography of breast lesions: Initial clinical results," *Radiology*, vol. 202, no. 1, pp. 79–86, Jan. 1997.
- [8] H. Rivaz, E. Boctor, P. Foroughi, R. Zellars, G. Fichtinger, and G. Hager, "Ultrasound elastography: A dynamic programming approach," *IEEE Trans. Med. Imag.*, vol. 27, no. 10, pp. 1373–1377, Oct. 2008.
- [9] G. R. Joldes, A. Wittek, and K. Miller, "Real-time nonlinear finite element computations on GPU—Application to neurosurgical simulation," *Comput. Methods Appl. Mech. Eng.*, vol. 199, no. 49, pp. 3305–3314, 2010.
- [10] D. Kotsianos-Hermle, S. Wirth, T. Fischer, K. M. Hiltawsky, and M. Reiser, "First clinical use of a standardized three-dimensional ultrasound for breast imaging," *Eur. J. Radiol.*, vol. 71, no. 1, pp. 102–108, Jul. 2009.
- [11] A. Fenster, G. Parraga, and J. Bax, "Three-dimensional ultrasound scanning," *Interface Focus*, vol. 1, no. 4, pp. 503–519, 2011.
- [12] S. Goenezen et al., "Linear and nonlinear elastic modulus imaging: An application to breast cancer diagnosis," *IEEE Trans. Med. Imag.*, vol. 31, no. 8, pp. 1628–1637, Aug. 2012.
- [13] W. A. Berg et al., "Shear-wave elastography improves the specificity of breast US: The BE1 multinational study of 939 masses," *Radiology*, vol. 262, no. 2, pp. 435–449, Feb. 2012.
- [14] O. Falou O et al., "Evaluation of neoadjuvant chemotherapy response in women with locally advanced breast cancer using ultrasound elastography," *Transl. Oncol.*, vol. 6, no. 1, pp. 17–24, Feb. 2013.
- [15] A. Sadeghi-Naini et al., "Quantitative ultrasound evaluation of tumor cell death response in locally advanced breast cancer patients receiving chemotherapy," *Clin. Cancer Res.*, vol. 19, no. 8, pp. 2163–2174, Apr. 2013.
- [16] L. Sannachi et al., "Non-invasive evaluation of breast cancer response to chemotherapy using quantitative ultrasonic backscatter parameters," *Med. Image Anal.*, vol. 20, no. 1, pp. 224–236, Feb. 2015.
- [17] S. R. Mousavi, H. Rivaz, A. Sadeghi-Naini, G. J. Czarnota and A. Samani, "Breast Ultrasound Elastography Using Full Inversion-Based Elastic Modulus Reconstruction," *IEEE Transactions on Computational Imaging*, vol. 3, no. 4, pp. 774–782, Dec. 2017.